

# RSC Advances



This is an *Accepted Manuscript*, which has been through the Royal Society of Chemistry peer review process and has been accepted for publication.

*Accepted Manuscripts* are published online shortly after acceptance, before technical editing, formatting and proof reading. Using this free service, authors can make their results available to the community, in citable form, before we publish the edited article. This *Accepted Manuscript* will be replaced by the edited, formatted and paginated article as soon as this is available.

You can find more information about *Accepted Manuscripts* in the [Information for Authors](#).

Please note that technical editing may introduce minor changes to the text and/or graphics, which may alter content. The journal's standard [Terms & Conditions](#) and the [Ethical guidelines](#) still apply. In no event shall the Royal Society of Chemistry be held responsible for any errors or omissions in this *Accepted Manuscript* or any consequences arising from the use of any information it contains.

# Silver incorporated antibacterial, cell compatible and bioactive titania layer on Ti metal for biomedical applications

Archana Rajendran and Deepak K. Pattanayak<sup>†</sup>

CSIR-Central Electrochemical Research Institute, Karaikudi, TamilNadu, 630006, India

## Abstract:

Surface modification of titanium and titanium alloy is one of the attractive methods to improve the biological affinity of orthopaedic and dental devices. Although osteointegration is enhanced by surface modifications, bacterial related infections sometimes lead to implant failure and secondary surgery. In the present study, attempts were made to incorporate antimicrobial agent silver into titanium metal pre-treated with H<sub>2</sub>O<sub>2</sub>. Fine nano network structures of hydrated titania uniformly formed by the H<sub>2</sub>O<sub>2</sub> treatment were decorated with silver particles of 5-10 nm by subsequent AgNO<sub>3</sub>, and, these silver particles remained stable over titania network even after heat treatment. Antibacterial study of titanium metal subjected to H<sub>2</sub>O<sub>2</sub>-AgNO<sub>3</sub> showed zone of inhibition in *Staphylococcus aureus* compared to H<sub>2</sub>O<sub>2</sub> pre-treated and untreated control specimen. Steady release of silver from thus treated titanium metals into simulated body fluid indicates that these silver particles are released as silver ions and are responsible for the antibacterial activity. About 99.7% bacterial killing efficiency was observed for 6-8 ppm (1mM AgNO<sub>3</sub>) silver containing Ti surface is optimised as the highest tolerable silver limit. The cytotoxicity assay and cell adhesion study on MG63 osteosarcoma cell lines confirmed the present silver concentration does not show any toxicity. Further, bone like apatite formation of chemically and heat-treated titanium in simulated body fluid indicates this surface modification method could be suitable in various medical devices.

**Keywords:** Surface modification, Chemical treatment, Orthopaedic implants, SBF; TEM.

---

<sup>†</sup>Corresponding author: Deepak K. Pattanayak; E-mail: deepak@cecri.res.in

## 1. Introduction

The bioactivity of an artificial material is the ability to induce the direct, adherent, and strong bonding with the surrounding bone tissues.<sup>1</sup> Metals such as Titanium (Ti) and Ti alloys are widely used as orthopaedic and dental devices because of their high mechanical strength, low elastic modulus, high corrosion resistance and good biocompatibility,<sup>2-5</sup> but they lack the bioactivity.<sup>6</sup> In order to improve the bone-bonding ability (bioactivity) of Ti and Ti alloys, various surface modification methods such as chemical treatment,<sup>7</sup> electrochemical treatment,<sup>8</sup> bioactive calcium phosphate coating by sol-gel,<sup>9</sup> chemical vapour deposition,<sup>10</sup> and biochemical modification<sup>11</sup> are reported. While comparing to other bioactive treatment methods, chemical solution treatment is simple, economical and can be applied to any porous and complicated metallic structure because of easy solution penetration and uniform chemical treatment.<sup>6, 12</sup>

Among various chemical treatment methods, Ti metal treated with NaOH solution at an elevated temperature forms sodium hydrogen titanate, a porous network structure on its surface.<sup>13, 14</sup> This network like morphology accelerates the bone-like apatite formation when soaked in simulated body fluid (SBF)<sup>15-17</sup> and forms new bone directly in contact with the implant surface in *in vivo*.<sup>18</sup> However, Na<sup>+</sup> ions released into the body might cause toxicity and cell death. Latter, it was found that the apatite formation can also be induced on NaOH treated Ti metal after hot water or dil HCl solution and heat treatment.<sup>19-21</sup> One of the author also proposed that Ti metal treated with mixed acid solution and heat treatment can induce bioactivity.<sup>22</sup> Recently, it has been reported that NaOH-HCl and the heat-treated Ti metal showed osteoconduction in dog muscle and this property is due to the surface positive charge formed during the treatments.<sup>23</sup> It was found that the pH of the surrounding solution plays a major role in apatite formation *in vivo* on the Ti metal surface. Results showed that either positive or negative

surface can induce bioactivity to Ti metal although mechanism of apatite-formation takes place in reverse manner.<sup>24</sup>

Apart from the above mentioned chemical treatment methods, hydrogen peroxide ( $\text{H}_2\text{O}_2$ ) treatment on Ti metal surface to provide a bioactive layer have also been widely investigated in recent years.<sup>25-27</sup> When Ti metal is treated with optimum concentration of  $\text{H}_2\text{O}_2$  solution at a moderate temperature and duration, able to provide a uniform micro porous network on its surface. Result suggests that  $\text{H}_2\text{O}_2 / \text{TaCl}_5$  treatment provides high bone-bonding ability and the implant has more shearing force compared to the untreated Ti metal when tested *in vivo*.<sup>25</sup> Wang et. al suggested that superoxide radicals formed during  $\text{H}_2\text{O}_2$  treatment are removed during the heat treatment at  $400^\circ\text{C}$ , which results in the formation of anatase layer that accelerates the apatite formation.<sup>26</sup> It is found that some metal ions are able to incorporate in this network structure formed on titanium surface by  $\text{H}_2\text{O}_2$  treatment and the success of incorporation depends upon the chemical state of oxygen or titanium atoms on its surface.<sup>27</sup> This metal ions are found to induce the apatite deposition while soaking in SBF. During osteoblast cells study, calcium and phosphate ions deposits on  $\text{H}_2\text{O}_2$  pre-treated samples indicate the new bone formation *in vitro*.<sup>28</sup> Shi et. al proposed that Ti alloy (Ti6Al4V) when treated with  $\text{H}_2\text{O}_2/\text{HCl}$  solution and heat-treated at  $400^\circ\text{C}$  forms a porous titania gel with increased bioactivity, enhanced proliferation and differentiation of osteoblast cells.<sup>29</sup> The mechanism of formation of nano porous titania gel on titanium surface during  $\text{H}_2\text{O}_2$  is also discussed elsewhere.<sup>30</sup>

Although the bioactivity can be given by the above mentioned chemical and thermal treatments, sometimes bacterial related infections caused during the surgery lead to the implant failure. Therefore, along with bioactivity if antibacterial property is provided by chemical solutions treatment, the risk of implant failure can be minimized. We recently reported that Ag

ions can be incorporated into the Ti metal when it is pre-treated with H<sub>2</sub>O<sub>2</sub> solution and thus formed Ag containing porous network structure shows antibacterial property.<sup>31</sup> Literatures also show that Ag incorporated Ti and Ti alloys pretreated with either H<sub>2</sub>O<sub>2</sub> or NaOH induce antimicrobial property.<sup>32, 33</sup> However, there is no substantial evidence on the effect of Ag on *in vitro* bioactivity of thus prepared Ti and Ti alloys. Further the stability of thus developed Ag containing titania layer without any heat treatment is under concern. A study on minimum concentration of Ag that can show antibacterial effect is essential in order to design/fabricate medical devices without any cytotoxicity. In addition, bioactivity of Ti metal in presence of silver in such an optimised condition is also essential.

In the present study, incorporation of optimum amount of Ag on Ti metal surface by chemical and thermal treatment that can induce antibacterial activity, cytocompatibility as well as bioactivity was carried out. Antibacterial activity was evaluated using *Staphylococcus aureus*, the major pathogenic bacteria that very often causes implant related infections. Based on the observation, the mechanism of antibacterial activity is proposed. Cytotoxicity and cell adhesion studies are also carried out for silver treated titanium surface on MG63, osteosarcoma cell lines. Bioactivity of chemically treated Ti metals in presence of silver is evaluated in simulated body fluid for different soaking periods.

## 2. Materials and methods

### 2.1 Preparation of the samples

Commercially pure Ti metal (CP Ti, Grade 2, Nilaco, Japan) was cut into rectangular samples with dimensions of 10 × 10 × 1 mm<sup>3</sup>, abraded with # 400 SiC paper, washed with acetone, 2-propanol, and ultra pure water for 15 min each in an ultrasonic cleaner, and then dried overnight in an oven at 40°C. Some samples were soaked in 10 mL of 27 % H<sub>2</sub>O<sub>2</sub> (Alfa aesar)

solution at 70°C in an oil bath, at 120 strokes / min for 3h and then gently washed with ultra pure water. The H<sub>2</sub>O<sub>2</sub> pre-treated samples were subsequently treated with AgNO<sub>3</sub> solution (Sigma Aldrich) of different concentrations in the range of 0.01-100 mM at 40°C for 3h and then gently washed with ultra pure water and allowed to dry.<sup>31</sup> Some of the samples were subjected to heat treatment at 600°C for 1h in normal atmospheric furnace. The rate of heating was maintained at 5° / min. Fig. 1 shows the schematic representation of various chemical and thermal treatments used in the present study. For TEM observation, Ti grids were directly used after treatment with H<sub>2</sub>O<sub>2</sub> solution and subsequently 0.05 and 100 mM AgNO<sub>3</sub> solution in the same method as described above. Notations of chemical treatments are listed in Table 1.

## 2.2 Surface analysis of the treated Ti metals

The surfaces of the Ti metals subjected to various chemical treatments described above were observed using scanning electron microscope (SEM; TESCAN, Czech Republic). The composition of chemically treated Ti metal surfaces were analysed by energy dispersive X-ray analysis (EDX) attached to the SEM under an acceleration voltage of 15kV. This analysis was carried out in two different location of each sample and averaged to know the amount of silver ions incorporated to the Ti metal surface.

X-ray diffraction (XRD) analysis was carried out to set the differences in the crystallographic structure for Ti-HP, Ti-HP-H600, Ti-HP-0.05-100Ag, Ti-HP-0.05-100AgH600 samples and compared with the untreated Ti metal. XRD measurements were made on a Bruker D8 Advance diffractometer in with Cu K $\alpha$  radiation and detected using a Bruker Lynx Eye detector. XRD spectra were recorded in the range 20-50° 2 $\theta$  at a step size of 0.02°.

In order to identify the surface functional groups, laser Raman spectroscopy (RENISHAW Co., UK) was used for untreated Ti metal and Ti metal subjected  $\text{H}_2\text{O}_2$ , and different concentrations of silver nitrate. For this measurement He-Ne Laser with a wavelength of 630 nm was used.

Morphology of Ti metal subjected  $\text{H}_2\text{O}_2$  and  $\text{H}_2\text{O}_2\text{-AgNO}_3$  were observed under transmission electron microscope (TEM; Tecnai 20 G2 FEI, The Netherland). The specimen for TEM observation was prepared by directly taking Ti TEM grids and then subjected to chemical treatments as described in previous section. SAED pattern were also taken for each conditions. Chemical state and composition of Ag containing Ti metal after heat treatment was investigated by X-ray photoelectron spectroscopy (XPS; Thermo V G Scientific, UK). All XPS data presented here were acquired using Al  $K\alpha$  line 1486.6 eV. The photoelectrons were collected at an electron take off angle of  $45^\circ$ . Peak positions were then calibrated with respect to the  $\text{C}_{1s}$  peak at 284.5eV.

Total amount of silver incorporated in to the Ti metal and the silver release in simulated body fluid (SBF) (detail method of preparation of SBF is explained in separate section.) was measured by atomic absorption spectroscopy (AAS; Varian Co., Australia). The network structure formed by  $\text{H}_2\text{O}_2\text{-AgNO}_3$  was dissolved in 10ml of 1 M HCl solution at  $70^\circ\text{C}$  for 3 hours and the resultant solution was making up to a final volume of 100 mL using ultra pure water. The silver ions present in the solutions were measured using standard solutions prepared in the range of 0.5-2ppm by AAS.

The concentration of silver ions released from the samples was also estimated in order to study the silver release kinetics. Here, Ti-HP-0.05Ag, Ti-HP-0.05Ag-H600 and Ti-HP-1Ag-H600 samples were first soaked in 50 mL of SBF. Each time 1 mL of SBF solution was drawn from the 50 mL and replaced with 1 mL fresh SBF so that the total volume remain constant. The

1 mL silver containing SBF solution was dissolved in equal amount of HNO<sub>3</sub> and then diluted 10 times and the amount of silver released were measured by AAS. All the samples were prepared in triplicates and average values obtained from the respective studies were statistically represented.

### 2.3 Antibacterial study

Disk diffusion and direct physical contact methods were used to evaluate the antimicrobial properties.

For disk diffusion method, 200 mL of nutrient medium was prepared with sterile distilled water in a conical flask and autoclaved at 121°C for 15min. Then at the hand bearable heat the sterilized nutrient medium was poured aseptically into the sterile petri plates and allowed to solidify. After solidification, the plates were kept in an inverted position to avoid the formation of water droplets inside the plates.<sup>31</sup> Lyophilized cells of *Staphylococcus aureus* were collected from Microbial Type Culture Collection and Gene Bank (MTCC), Dept. of Biotechnology, Chandigarh, India. The vials were cut open and the lyophilized cells were aseptically transferred into the nutrient broth (0.5% NaCl, 0.15% yeast extract, 0.15% beef extract, 0.5% peptone) at room temperature for about 24h. The overnight culture of *Staphylococcus aureus* was prepared at a concentration of 10<sup>5</sup> colony forming unit (CFU / mL) and around 100 µl were evenly spreaded over the nutrient agar plates using sterile cotton swab. All the treated Ti metal plates were aseptically placed on the inoculated plates using a sterile forceps and incubated for 24 h.<sup>31</sup>

For direct physical contact method, a bacterial solution of 10<sup>6</sup> CFU / mL was prepared and 100 µl of the bacterial solution was introduced on to the surface of Ti-HP-0.05-100Ag-H600 samples (10 x 10 x 1mm<sup>3</sup>). The samples were then incubated at 37°C without any disturbance. After 6 h



of incubation, the surface attached cells were carefully removed by washing with ultra pure water and the final volume was made up to 1 mL cell solution. Spread plate was prepared using 100  $\mu$ L out of the above 1 mL collected cell solution from each sample surface to compare the effect of Ag concentration on antibacterial activity. Plates were incubated at 37°C in an incubator at static condition. After 24 h of incubation, the plates were collected and the colony formed was manually counted. The efficiency of bacterial killing was calculated by using the following equation,

$$[(Nc-Ns)/ Nc] \times 100\%$$

Where, Nc - average number cells in the control sample, Ns- average number of cells in the test sample.<sup>34</sup>

#### **2.4 Cytotoxicity and cell adhesion study**

The human MG-63 osteosarcoma cell line was purchased from NCCS Pune, India and maintained in Dulbecco's modified Eagle's medium (DMEM) with 10% fetal calf serum (FCS) and 1% gentamicin. Cultures were kept at 37°C in a humidified atmosphere of 5 % CO<sub>2</sub> and 95 % air. 80 % of the confluent cells were detached from the culture flask through trypsinisation process, centrifuged to separate the media and re-suspended in fresh medium.

#### **MTT assay**

In order to evaluate the cytocompatibility of chemically treated samples, MTT assay was performed. MTT assay is based on the metabolic ability of the viable cells to reduce soluble MTT by mitochondrial enzyme into an insoluble color formazan product, which is measured spectrophotometrically.<sup>35</sup> The insoluble formazan was dissolved in dimethylsulfoxide (DMSO)

before subjecting it for spectrophotometric measurement at an wavelength of 570nm. The samples were UV sterilized for 15 min and placed inside a 24-well culture plate. Subsequently, 500  $\mu$ l of cell suspension containing about 15,000 cells were seeded on the sample containing wells. Well loaded with cells, without samples, served as the control and considered as 100% viability. Cells were incubated in a CO<sub>2</sub> incubator at 37°C, 5% CO<sub>2</sub> and 95% air. The culture medium was removed and the cells were washed twice with sterile phosphate buffer solution (PBS). The cells were incubated with 250  $\mu$ l PBS containing MTT (0.5 mg / ml) in a CO<sub>2</sub> incubator at 37°C (5% CO<sub>2</sub> and 95% air). After 3 h of incubation, the PBS was removed and the formazan product formed was solubilised in 150  $\mu$ l of DMSO. The absorbance was measured at 570 nm using BioRadmicroplate reader.<sup>36</sup> Each experiment was performed in triplicate and the average value was statistically represented.

### **Cell adhesion study**

In order to study the morphology of cells adhered on Ag treated Ti surface, cells were allowed to grow on the surface and was observed under SEM after proper fixation. Briefly 20,000 cells (MG63) were seeded on sample surface without overflowing and incubated in a CO<sub>2</sub> incubator at 37°C, 5% CO<sub>2</sub> and 95% air for 24 h. After incubation the cells on the sample surface were fixed with 4% w/w formaldehyde in PBS and incubated for 30 min at room temperature. Further the cells were dehydrated through a series of ethyl alcohol solution (from 50 % to 100 % v/v in distilled water), followed by a ratio of ethyl alcohol and hexamethyl disilazane solution at 3:1, 1:1 and 1:3 ratios respectively. Samples were air dried and observed in SEM after gold sputtering.

## 2.5 Preparation of simulated body fluid (SBF) and *invitro* bioactivity study

SBF is an acellular solution with ion concentrations nearly equal to those of human blood plasma at 36.5°C. The SBF was prepared by dissolving reagent-grade NaCl, NaHCO<sub>3</sub>, KCl, K<sub>2</sub>HPO<sub>4</sub>·3H<sub>2</sub>O, MgCl<sub>2</sub>·6H<sub>2</sub>O, CaCl<sub>2</sub> and Na<sub>2</sub>SO<sub>4</sub> (Sigma Aldrich) into ultra-pure water, and buffered at pH 7.4 with tris-hydroxymethylaminomethane ((CH<sub>2</sub>OH)<sub>3</sub> CNH<sub>2</sub>) and 1M HCl (Sigma Aldrich).<sup>37</sup> Subsequently the SBF was kept in a refrigerator for 3 to 4 days before using for the study.

### In vitro bioactivity in SBF

Each specimen subjected to chemical treatment or chemical and thermal treatment are immersed in 30 mL of SBF contained polypropylene centrifuged bottles covered with a tight lid and kept in a water bath maintained a temperature of 36.5°C for 1 and 7 days. After the specified duration, the samples were removed from the solution, gently washed with distilled water and dried for further characterization. The morphology of bone-like apatite formation on the surface of Ti metal surface during the incubation was observed using SEM and presence of apatite peaks were confirmed by XRD. All samples were coated with gold prior to SEM observation.

## 3. Results and discussions

Fig. 2 shows the SEM images of Ti metal as-polished (control) and treated with H<sub>2</sub>O<sub>2</sub> and subsequently in AgNO<sub>3</sub> solution of different concentrations. It can be seen from Fig. 2 that as-polished Ti metal had smooth surface apart from few scratches formed during the polishing with # 400 grade SiC paper. However, on subsequent treatment with H<sub>2</sub>O<sub>2</sub> solution surface became rough with the formation of porous network like structure due to the chemical reaction between H<sub>2</sub>O<sub>2</sub> and Ti metal. This indicates that after H<sub>2</sub>O<sub>2</sub> treatment the Ti metal surface form hydrated titania layer with porous network structure in nanometer scale which covers the entire surface.

On subsequent treatment with  $\text{AgNO}_3$  solution, this porous network structure remained stable irrespective of  $\text{AgNO}_3$  concentrations. However, few cracks were observed on the surface of the Ti metal after  $\text{H}_2\text{O}_2$  treatment and remained even after  $\text{AgNO}_3$  treatment. This may be due to the shrinkage of the porous network structure when the samples were allowed to dry.<sup>38</sup> The surface morphology of porous network structure remained unaffected even after the heat treatment at  $600^\circ\text{C}$  for 1 h (Ti-HP-100Ag-H600) and is shown in Fig. 2. This porous hydrated titania surface structure is expected to encapsulate silver ions into the networks. In order to confirm the presence of silver in the porous network surface after chemical treatments, energy dispersive X-ray analysis (EDX) was carried out.

Fig. 3 (a) represents the elemental composition of silver deposited on the Ti-HP-0.05-100Ag and a magnified image is shown in the inset. Results showed that silver nitrate at a concentration ranging from 0.05 to 100 mM were able to incorporate 0.64 to 3.77 at.% of silver on Ti-HP surface. The silver incorporation on the surface of Ti-HP samples increased rapidly up to 1 mM  $\text{AgNO}_3$  concentration and attained saturation. This indicates that the protons ( $\text{H}^+$  ions) present on the porous hydrated titania layer are easily replaced by the silver ions. Even though EDX can measure the elements up to a depth of  $2\ \mu\text{m}$ , it may not be effective to calculate the total silver incorporated into the entire Ti metal surface (possibility of silver entrapped inside the porous networks). Therefore, in order to evaluate the total silver deposited on Ti surface, the network structure was completely dissolved by 1 M HCl solution and the amount of silver was quantified by AAS. Fig. 3 (b) shows the graphical representation of total silver present in the Ti-HP-1-100Ag samples. It can be seen from Fig 3 (b) that 3 ppm silver was incorporated for 0.01 mM  $\text{AgNO}_3$  (Ti-HP-0.01Ag) sample and attained a saturation above 1 mM  $\text{AgNO}_3$  solution. This indicates that maximum amount of silver that can be incorporated was in the range of 6-8

ppm by this chemical treatment method. At higher silver concentration (10-100mM AgNO<sub>3</sub>) there is a possibility of existence of silver particles on chemically treated Ti surface. Thus incorporated silver and its toxicity to bacteria and osteoblast cells will be discussed in later sections.

TEM was used to investigate the size and distribution of silver deposits on the chemically treated Ti metal. The variation in the morphology of the surface deposited silver after heat treatment was compared with that of samples before heat treatment. Fig. 4 shows the TEM images of Ti-HP, Ti-HP-0.05Ag, Ti-HP-0.05Ag-H600, Ti-HP-100Ag, Ti-HP-100Ag-H600 and the corresponding SAED pattern were shown in the inset. TEM image showed that H<sub>2</sub>O<sub>2</sub> treatment forms sheet like morphology of 100-200nm in length on the entire surface and corresponding SAED pattern indicated that the H<sub>2</sub>O<sub>2</sub> treated surface is in amorphous phase (Fig. 4(a)). Subsequent treatment with AgNO<sub>3</sub> solution, the silver particles were uniformly deposited on the sheet like structures which is clearly seen in Ti-HP-100Ag sample compared to Ti-HP-0.05Ag (Fig. 4 (b) and (d)). This indicates that the Ag incorporated into hydrated titania gel layer took the shape of particles during the chemical treatment. The size of the silver particles ranges from 2 to 5 nm. Fig. 4(c) and (e) shows the silver deposited samples after heat treatment. Long sheet like structure as seen in Fig. 4(a) took the shape of particulate morphology where silver particles (5-10 nm) are decorated on its surface. The silver particle size was increased after heat treatment possibly due to the agglomeration on the TiO<sub>2</sub> surface. SAED pattern showed that heat treatment at 600°C forms a crystalline titania.<sup>39, 31</sup> From the TEM observation it can be speculated that silver ions from AgNO<sub>3</sub> solution replaces the protons and these silver ions are easily transformed to silver particles in presence of water and light (before heat treatment sample). These silver particles grow by agglomeration and appeared bigger particles on heat

treatment. However, there is a possibility of presence of silver ions in titania layer. In order to understand the state of silver, XPS analysis of Ti-HP-0.05AgH600 was carried out and is shown in Fig. 5. The survey scan shows the presence of oxygen, titanium and silver along with carbon peak. Narrow scan of  $\text{Ag}_{3d}$  peak is shown as an inset. Peak corresponding to 367.8eV ( $\text{Ag}^+$ ) indicates silver to be present as  $\text{Ag}_2\text{O}$ . Additional broad peak at 368.2 is assigned to be  $\text{Ag}^0$  state (indicates the presence of trace amount of metallic silver).  $\text{Ag}^0$  peak might be clearer for 100mM  $\text{AgNO}_3$  treated sample (not shown here) as TEM observation showed large agglomerated particles (Fig. 4 (e)). It is well known that silver on titania surface can easily oxidised in to silver oxide ( $\text{Ag}_2\text{O}$ ).

Fig. 6 shows Raman spectra of Ti metal untreated and treated with  $\text{H}_2\text{O}_2$  and various concentrations of  $\text{AgNO}_3$  solution. The untreated Ti metal showed no characteristic peaks due to its metallic nature. However, after  $\text{H}_2\text{O}_2$  treatment, hydrated titania peaks appeared at 288, 527, 680 and 915  $\text{cm}^{-1}$ .<sup>20</sup> This indicates that  $\text{H}_2\text{O}_2$  readily reacts with Ti metal and forms the hydrated titania on the surface of Ti metal. This layer appeared to be porous network structure as seen in Fig.2. All the peaks remained same even after  $\text{AgNO}_3$  treatment, although incorporation of silver is confirmed by EDX.

On subsequent heat treatment these hydrated titania gel like layer was transformed to anatase phase as confirmed by the peaks at 402, 518, 644  $\text{cm}^{-1}$  in Raman spectra (Fig.7 (a)). Further, XRD spectrum showed a peak at 25 in 2 theta that corresponds to anatase phase as seen in Fig. 7(b) and (c) and the peak position was not affected by the subsequent  $\text{AgNO}_3$  treatment. No  $\text{Ag}_2\text{O}$  peak was observed in XRD possibly due to the presence of very limited silver amount although, XPS (Fig. 5) clearly shows the peak due to high sensitivity of the instrument. Along with anatase some amount of rutile phase was also observed. Pure Ti metal when heat treated

form only rutile phase as shown in Raman and XRD peaks.<sup>40</sup> No silver peak was observed possibly due to less concentration and below the detectable limit of the instrument.

Fig. 8 shows the release rates of silver from Ti-HP-0.05Ag, Ti-HP-0.05Ag-H600 and H<sub>2</sub>O<sub>2</sub>-1Ag-H600 samples in simulated body fluid with respect to time as measured by AAS. In case of Ti-HP-0.05Ag sample the amount of silver release increased from 0.72 to 1.71 ppm within 1 h and it reached 2.1 ppm in 3 h. This indicates that the initial release rate of silver was high and it became almost stable after 7 days. Initial high release of the silver is expected to favour rapid killing of bacterial cells and prevents the formation of biofilm. If the initial release rate is slow, there is a possibility to develop resistance against the antibacterial agent by the bacteria. Surprisingly, the release rate of silver for heat treated sample (Ti-HP-0.05Ag-H600) was decreased from 0.72 to 0.16 ppm. However, Ti-HP-1Ag-H600 sample showed similar silver release kinetics to that of Ti-HP-0.05Ag sample.

Steady and stable release of silver over long periods of time helps in maintaining the long term antibacterial effect of the medical devices. Silver release from Ti-HP-Ag sample shows similar trend as that of the silver nanoparticles.<sup>41</sup> Since SBF is having the similar ionic composition of human blood plasma, we can assume that a same trend of silver release can happen when the material is implanted inside the human body. In the initial release time surface bonded silver are released in to the SBF. On increasing the soaking time the silver encapsulated in between the network structures will release in sustainable rate. Release of silver ions from Ti-HP-Ag samples also depends upon its diffusion behaviour. In addition the silver ion release is also governed by the concentration of silver on the surface and crystallinity of the material. The phase of the material depends upon the temperature at which it is processed.

Fig. 9 (a) and (b) shows the bacterial zone of inhibition study of Ti-HP-0.05-100Ag before and after heat treatment against *Staphylococcus aureus*. It can be seen that the pure Ti metal (control) and H<sub>2</sub>O<sub>2</sub> treated Ti metal did not show any inhibition zone. This indicates that *Staphylococcus aureus* is resistant to Ti metal with hydrated titania layer or anatase layer formed by H<sub>2</sub>O<sub>2</sub> solution and heat treatment, respectively. It has already been reported that *Staphylococcus aureus* can survive in a solution containing sodium titanate without any silver ions.<sup>31, 42</sup> In the present study, similar observation was made even for hydrated titania layer on Ti metal.<sup>31</sup> However, this hydrated titania layer incorporated with silver ions shows excellent antibacterial activity which is observed from the zone of inhibition in Fig. 9 (a). All the silver treated Ti samples showed zone of inhibition. We examined in the range of 0.05-100 mM concentration of silver nitrate samples (3-8 ppm silver on the Ti surface) in order to understand the minimum concentration of silver which can show antibacterial property against *Staphylococcus aureus*. (Gram negative bacteria *E. coli* (not shown here), was studied and results showed similar trend like *S. aureus*). The minimum silver concentration that can show zone of inhibition against *Staphylococcus aureus* was 0.05 mM AgNO<sub>3</sub> solution. This indicates that the silver containing hydrated titania formed during the silver nitrate treatment is able to release the silver when come in contact with any fluid.<sup>41</sup> In the disk diffusion method the moisture present in the nutrient agar plates helps the silver particles to diffuse from the Ti surface as silver ions (Ag<sup>+</sup>) and inhibits the bacterial growth on the sample surrounding. However, heat treated samples with similar AgNO<sub>3</sub> concentration did not show any antibacterial activity. On the other hand, silver concentration above 1 mM showed the zone of inhibition after heat treatment [Fig. 9 (b)]. This indicates that antibacterial activity is directly related to the rate of silver release from each sample surface. As evident from AAS, the release rate of silver decreased after heat



treatment but the trend of release remained same. The decrease in release rate indicates the formation of a stable silver containing titania phase by the subsequent heat treatment. In case of heat treated samples, sufficient inhibition zone was not found during disk diffusion method. After heat treatment there is a possibility that silver particles incorporated to the titania layer on Ti becomes more stable. This decreased the amount of Ag release to the surrounding environment although same amount of silver was present on the sample surface. In such case instead of disk diffusion method, a direct physical contact method was used.

Fig. 9 (c) shows the images of spread plate prepared from the bacterial solution from the surfaces of Ti-HP-0.05Ag-H600, Ti-HP-1Ag-H600, Ti-HP-10Ag-H600, Ti-HP-100Ag-H600 samples. All the samples were compared with the control samples and Ti-HP-H600 sample plates. For control sample and Ti-HP-H600 sample (result not shown here), similar trend of bacterial growth was observed. We studied the effect of silver release for bactericidal activity for the initial 6 h. For the silver incorporated samples, the number of bacterial cells was decreased after 6 h, compared to the control samples. This is due to the effect of silver ions released from the sample surface during the incubation time. In an ideal antibacterial biomaterial, the initial rapid release of silver, followed by a sustained lower release improves its efficacy, which has been proved by earlier reports.<sup>43</sup> Bacterial killing efficiency for Ti-HP-0.05Ag-H600, Ti-HP-1Ag-H600, Ti-HP-10Ag-H600, Ti-HP-100Ag-H600 samples were also calculated from counting the CFU / ml for each spread plates. The percentage of killing efficiency is given in Table. 2. The data showed that Ti-HP-1Ag-H600, Ti-HP-10Ag-H600, Ti-HP-100Ag-H600 is having 99% of killing efficiency. Ti-HP-0.05Ag-H600 sample is having little less, 89% of killing efficiency. Based on these results, Ti-HP-1Ag-H600 was found to be the highest tolerable silver

concentration among the test specimens. The cytocompatibility studies of Ti-HP-1Ag-H600 is discussed in the latter section.

The possible mechanism in which the silver ion kills the bacteria is schematically represented in Fig. 10. The silver ion binds to the bacterial cell wall through some electrostatic attraction and thus destroys the integrity of cell membrane. This affinity of silver ions are already discussed elsewhere.<sup>44</sup> The positive charge of the silver ions may be the reason for these electrostatic attractions.<sup>44</sup> Reports suggests that silver is able to bind to the thiol functional group in the protease enzyme present in the membrane. This disturbs the membrane equilibrium and ultimately destroys the membrane.<sup>31, 45</sup>

Although presence of silver on Ti metal kills the bacteria, it is essential to estimate the amount of silver i.e. 3 to 8 ppm and its toxicity to bone cells. MTT assay was studied in MG63 osteosarcoma cell lines and the result is shown in Fig.11. The absorbance of cell intensity measured at 570 nm is converted in to percentage, were plotted against the sample condition as in Fig.11. The viability of control cells, without any samples, was considered as 100%. Ti-HP-H600 is considered as the samples control. Compared to Ti-HP-H600, all the samples in the range of 0.01-1mM showed a viability of above 80% MG63 cells. From the quantification studies and antibacterial studies (Fig. 3 (a), (b), Fig. 8, Fig 9. (a)-(c)) we found that, Ti-HP-1Ag-H600 is having nearly saturated amount of silver on its surface. And also for antibacterial activity it is shown the similar bactericidal property compared to the Ti-HP-10AgH600 and Ti-HP-100Ag-H600 samples. As evident from AAS data around 6.7 ppm of silver is present in Ti-HP-1Ag-H600 samples. An earlier report says that around 10 ppm of silver is acceptable to human body and above that it may cause severe health effects including neuropathy.<sup>46</sup> A detailed study on the pharmacological and toxicological limit of silver was also reported previously.<sup>47</sup>

However, the exact amount of silver that can lead to toxicity of human cells is still unknown. The present amount of silver is sufficient to show antibacterial activity towards *S. aureus*. From the MTT assay the cell viability of Ti-HP-1Ag-H600 is 89.37%, shows this sample is not toxic to MG63 cells. Fig. 11 (b) shows MG63 cells adhered to Ti-HP-1Ag-H600 sample surface. Cells were uniformly adhering to the surface within 28 h of incubation and most of the cells showed random spreading. Cell attachment, spreading and further proliferation is directly related to surface characteristics of the material.<sup>48</sup> The adherence of MG63 cells to the Ti-HP-1Ag-H600 surface indicate that the current surface is biocompatible and induce further proliferation of the cells.

Presence of silver along with anatase surface might affect the bioactivity of Ti metal although compared to simple anatase containing Ti metal.<sup>26</sup> Therefore, it is essential to examine the bioactivity of this silver containing titanium samples in physiological body conditions. Fig. 12 shows the bioactivity study of Ti metal samples chemically treated with H<sub>2</sub>O<sub>2</sub> and AgNO<sub>3</sub> and subsequently heat treated at 600 °C, soaked in SBF for a period of 1 and 7 days. Results showed that pure Ti metal heat treated at 600°C without any chemical treatment did not form any apatite (spherical particles) even after 7 days. However Ti metal after H<sub>2</sub>O<sub>2</sub> and heat treatment formed apatite within 1 day. It can be seen that the surface is fully covered with apatite even for Ti-HP-0.05-100Ag-H600. After the silver ion incorporation in titania gel layer, it seems that the trend of apatite formation increased with increase in silver content.

Fig. 13 shows the XRD pattern of the surfaces of Ti metal after being treated with Ti-HP-H600, Ti-HP-0.05-100Ag-H600 and soaked in an SBF for a period of 7 days. The spherical particles observed on the surfaces of Ti metal in Fig. 10 are identified as being bone-like apatite (Peaks at 26 and 32) from XRD pattern. Ti metal (control) subjected to heat treatment did not

form any apatite on its surface. This indicates that present surface modification method improve the bioactivity (apatite formation) of Ti metal. It has been shown for various bioactive ceramics and glasses that a material able to form bone-like apatite on its surface in an SBF generally form apatite on its surface in the living body and bonds to living bone through the apatite layer.<sup>22, 32</sup> Based on same principle, later it was found that Ti metal could also form apatite on its surface in the living body and bond to living bone through this apatite layer if surface of Ti metal is treated with NaOH<sup>14, 15, 18</sup>, NaOH-HCl<sup>6, 19</sup>, mixed acid<sup>22, 23, 49</sup> and then heat treatment.

Earlier, one of the author reported that Ti metal exhibits a surface charge of around zero in body environment even after heat treatment<sup>24</sup> and does not form apatite on its surface. Similar observation was made in the present study. Ti metal when treated with H<sub>2</sub>O<sub>2</sub> forms hydrated titania layer on its surface. When heat-treated at 600°C, this hydrated titania is converted to anatase layer. This anatase layer induces the deposition of apatite on its surface. Ohtsuki et. al reported that the basic Ti-OH group in titania hydrogel formed during the H<sub>2</sub>O<sub>2</sub> treatment induce the apatite nucleation and growth.<sup>27</sup> Similar observation were made in the present study as seen in Fig. 12. Heat treatment is essential to improve the scratch resistance of chemically treated Ti metal compared to before heat treatment.<sup>20</sup>

Present study also shows that the apatite-forming ability of H<sub>2</sub>O<sub>2</sub> treated Ti metal is also not affected by the subsequent AgNO<sub>3</sub> treatment. This indicates that release of Ag<sup>+</sup> ions as observed by AAS in Fig. 8 triggers the apatite forming ability of H<sub>2</sub>O<sub>2</sub>-AgNO<sub>3</sub> and heat-treated Ti metal by forming surface Ti-OH groups.<sup>24</sup> Thus it can be expected that silver ion release into SBF serve two purposes. First silver release accelerates the apatite formation by forming Ti-OH groups and second the released silver ion kills the bacteria surrounding the Ti metal (implant). It was noticed from Fig. 8 that Ag<sup>+</sup> ions are strongly bonded to titania layer when subjected to heat

treatment compared to before heat treatment sample. Silver release from the surface of sample is essential for antibacterial activity as seen from zone of inhibition result in Fig. 9. Based on the observation, mechanism of antibacterial activity is proposed schematically in Fig.10. Wang et al also reported that  $\text{Ag}^+$  ion incorporated into the NaOH treated Ti metal showed antibacterial activity but they did not discuss about the bioactivity of thus treated Ti metal in presence of  $\text{Ag}^+$  ion.<sup>50</sup> Present observation showed both antibacterial activity as well as bioactivity of Ti-HP-0.05-100Ag and Ti-HP-0.05-100Ag-H600. The concentration of Ag that can show highest tolerable silver concentration is optimised to be Ti-HP-1Ag-H600. It is well known that excess silver is toxic and can lead to cell death. Cell cytotoxicity and cell adhesion studies as explained in the present study further confirmed that the present optimised concentration of silver has no toxic effects on MG63 osteosarcoma cells.

## Conclusion

Silver particle of different silver concentrations could be successfully incorporated into Ti metal pre-treated with  $\text{H}_2\text{O}_2$ . Fine nano network structures of hydrated titania layer was uniformly formed by the  $\text{H}_2\text{O}_2$  treatment and remained stable even after subsequent  $\text{AgNO}_3$  solution. Silver decorated on the nano network structures as silver particles of 5-10 nm in diameter, and, these silver particles remained stable even after heat treatment. Antibacterial study of titanium metal subjected to  $\text{H}_2\text{O}_2$ - $\text{AgNO}_3$  showed zone of inhibition in *Staphylococcus aureus* compared to  $\text{H}_2\text{O}_2$  pre-treated and untreated control specimen. Steady release of silver ions from thus treated titanium metals into simulated body fluid is responsible for the antibacterial activity. The detailed antibacterial study on heat treated silver incorporated Ti samples proved around 99% bacterial killing efficiency for 6 to 8 ppm silver incorporation is optimised as the highest tolerable silver concentration. Cell cytotoxicity and cell adhesion studies confirmed that the

present optimised concentration of silver has no toxic effects on MG63 osteosarcoma cells. Further, apatite-formation of chemically and heat-treated titanium in SBF indicates the surface modification method to be suitable in various orthopaedic and dental devices.

### Acknowledgements

Present authors would like to acknowledge Dr. S. Maruthamuthu for providing facilities for antibacterial study. Research grant from Department of Science and Technology (DST), NewDelhi, India (SERB; Fast track research grant no SB/FTP/ETA-257/2012, GAP 11/13) and support from Central Instrument Facility staff Mr. A. Rathish Kumar (TEM in charge), Mr. R. Ravishankar and Ms. Nalini (SEM in charge) CSIR-CECRI, Karaikudi is greatly appreciated. AR acknowledges DST for providing the fellowship to carry out the work. Preliminary cell cytotoxicity and cell adhesion studies by Dr. M. Kiran Kumar at CSIR-CLRI, Chennai, are highly acknowledged.

### References

- 1 L. L. Hench, *J. Am. Cer. Soc.*, 1991, **74**, 1487–1510.
- 2 T. Kokubo, *Bioceramics and their clinical applications*, Cambridge:Woodhead publishing Ltd.,2008.
- 3 T. Kokubo, H. M. Kim, M. Kawashita and T.Nakamura, *J. Mater. Sci.: Mater. Med.*, 2004, **15**, 99-107.
- 4 M. Niinomi, *Metals for biomedical devices*, Cambridge, Woodhead Publishing Ltd., 2010.
- 5 D. M. Brunette, P. Tengvall, M. Textor and P. Thomsen, *Titanium in Medicine, Material Science, Surface Science, Engineering, Biological Responses and Medical Applications*, Springer, Germany 2001.

- 6 D. K. Pattanayak, A. Fukuda, T. Matsushita, M. Takemoto, S. Fujibayashi, K. Sasaki, N. Nishida, T. Nakamura and T. Kokubo, *ActaBiomater.*, 2011, **7**, 398-406.
- 7 X. Y. Liu, P. K. Chu and C. X. Ding, *Mater. Sci. and Eng. R.*, 2004, **47**, 49-121.
- 8 B. Yang, M. Uchida, H. M. Kim, X. Zhang and T. Kokubo, *Biomaterials*, 2004, **25**, 1003-1010.
- 9 J. X. Zhang, R. F. Guan and X. P. Zhang, *J. Alloys and Compounds*, 2011, **509**, 4643-4648.
- 10 M. V. Cabanas, M. Vallet-Regi, *J. Mater. Chem.*, 2003, **13**, 1104-1107.
- 11 M. Weber, A. Vasella, M. Textor and N. D. Spencer, *Helvetica ChimicaActa.*, 1998, **81**, 1359-1372.
- 12 A. Fukuda, M. Takemoto, T. Saito, S. Fujibayashi, M. Neo, D. K. Pattanayak, T. Matsushita, K. Sasaki, N. Nishida, T. Kokubo and T. Nakamura, *ActaBiomater.*, 2011, **7**, 2327-2336.
- 13 T. Kokubo, F. Miyaji and H. M. Kim, *J. Am. Ceram. Soc.*, 1996, **79**, 1127-1129.
- 14 H. M. Kim, F. Miyaji, T. Kokubo and T. Nakamura, *J. Biomed. Mater. Res.*, 1996, **32**, 409-417.
- 15 H. M. Kim, F. Miyaji and T. Kokubo, *J. Mater. Sci.: Mater. Med.*, 1997, **8**, 341-347.
- 16 H. B. Wen, J. R. de Wijn, F. Z. Cui and K. De Groot, *Biomaterials*, 1998, **9**, 215-221.
- 17 H. B. Wen, Q. Liu, J. R. de Wijn, K. de Groot, *J. Mater. Sci.: Mater. Med.*, 1998, **9**, 121-128.
- 18 W. Q. Yan, T. Nakamura, K. Kawanabe, S. Nishigochi, M. Oka and T. Kokubo, *Biomaterials*, 1997, **18**, 1185-1190.

- 19 M. Takemoto, S. Fujibayashi, M. Neo, J. Suzuki, T. Matsushita, T. Kokubo and T. Nakamura, *Biomaterials*, 2006, **27**, 2682-2691.
- 20 D. K. Pattanayak, T. Kawai, T. Matsushita, H. Takadama, T. Nakamura, and T. Kokubo, *J. Mater. Sci.: Mater. Med.*, 2009, **20**, 2401-2411.
- 21 D. K. Pattanayak, S. Yamaguchi, T. Matsushita and T. Kokubo, *J. Mater. Sci.: Mater. Med.*, 2011, **22**, 1803-1812.
- 22 T. Kokubo, D. K. Pattanayak, S. Yamaguchi, H. Takadama, T. Matsushita, T. Kawai, M. Takemoto, S. Fujibayashi and T. Nakamura, *J. R. Soc. Inter.*, 2010, **7**, S503–S513.
- 23 T. Kawai, M. Takemoto, S. Fujibayashi, H. Akiyama, M. Tanaka, S. Yamaguchi, D.K. Pattanayak, K. Doi, T. Matsushita, T. Nakamura, T. Kokubo and T. Matsuda, *Plos one*, 2014, **9**, e88366.
- 24 D. K. Pattanayak, S. Yamaguchi, T. Matsushita, T. Nakamura, and T. Kokubo, *J. R. Soc. Inter.*, 2012, **9**, 2145-2155.
- 25 S. Kaneko, K. Tsuru, S. Hayakawa, S. Takemoto, C. Ohtsuki, T. Ozaki, H. Inoue and A. Osaka, *Biomaterials*, 2001, **22**, 875-881.
- 26 X. X. Wang, S. Hayakawa, K. Tsuru and A. Osaka, *J. Biomed. Mater. Res.*, 2000, **52**, 171-176.
- 27 C. Ohtsuki, H. Iida, S. Hayakawa and A. Osaka, *J. Biomed. Mater. Res.*, 1997, **35**, 39-47.
- 28 J. Pan, H. Liao, C. Leygraf, D. Thierry and J. Li, *J. Biomed. Mater. Res.*, 1998, **40**, 244-256.
- 29 G. S. Shi, L. F. Ren, L. Z. Wang, H. S. Lin, S. B. Wang and Y. Q. Tong, *Oral Surgery, Oral Medicine, Oral Pathology, Oral Radiology and Endodontology*, 2009, **108**, 368-375.
- 30 M. Wen, J. F. Gu, G. Liu, Z. B. Wang and J. Lu, *Appl. Surf. Sci.*, 2008, **254**, 2905-2910.



- 31 A. Rajendran, G. Vinoth, V. Shanthi, R. C. Barik and D. K. Pattanayak, *Mater. Technol. Adv. Biomater.*, 2014, **29**, B26-B34.
- 32 S. Ferraris, A. Venturello, M. Miola, A. Cochis, L. Rimondini and S. Spriano, *App. Surf. Sci.*, 2014, **311**, 279-291.
- 33 N. Ren, R. Li, L. Chen, G. Wang, D. Liu, Y. Wang, L. Zheng, W. Tang, X. Yu, H. Jiang, H. Liu and N. Wu, *J. Mater. Chem.*, 2012, **22**, 19151-19160.
- 34 J. Li, Y. Qiao, H. Zhu, F. Meng, and X. Liu, *Int. J. Nanomedicine* , 2014, **9**, 3389-3402.
- 35 D. Gerlier and N. Thomasset, *J. Immunological Methods*, 1986, **94**, 57-63.
- 36 W. Chrzanowski, N. E. A. Abou, D. A. Armitage, X. Zhao, J. C. Knowles and V. J. Salih, *J. Biomed. Mater. Res. Part A.*, 2010, **93**, 1596-1608.
- 37 T. Kokubo and H. Takadama, *Biomaterials*, 2006, **27**, 2907-2915.
- 38 M. Karthega, S. Nagarajan and N. Rajendran, *Electrochimica Acta.*, 2010, **55**, 2201-2209.
- 39 V. Vamathevan, R. Amal, D. Beydoun, G. Law and S. McEvoy, *Chem. Eng. J.*, 2004, **98**, 127-139.
- 40 X. Sun and Y. Li, *Chem. Eur. J.*, 2003, **23**, 2229-2238.
- 41 S. B. Lee, U. Otgonbayar, J. H. Lee, K. M. Kim, and K. N. Kim, *Surf. Coating and Technol.*, 2010, **205**, S172-S176.
- 42 C. Zhao, B. Feng, Y. Li, J. Tan, X. Lu and J. Weng, *Appl. Surf. Sci.*, 2013, **280**, 8-14.
- 43 K. J. Thevi, S. A. Bakar, S. Ibrahim, N. Shahab and M. R. M. Toff, *Vacuum*, **86**, 2011, 235-241.
- 44 A. Thill, O. Zeyons, O. Spalla, F. Chauvat, J. Rose, M. Auffan and A. M. Flank, *Environ. Sci. Technol.* 2006, **40**, 6151-6156.

- 45 Y. H. Su, Z. F. Yin, H. L. Xin, H. Q. Zhang, J. Y. Sheng, Y. L. Yang, J. Du and C. Q. Ling, *Int.J.Nanomedicine*, 2011, **6**, 1579-1586.
- 46 H. Vik, K. J. Andersen, K. Julshamn and K. Todnem, *Lancet*, **1**, 1985, 872.
- 47 A. B. G. Lansdown, *Advances in Pharmacological Sciences*, **2010**, 1-16 .
- 48 B. H. Zhao, I. S. Lee, I. H. Han, J. C. Park, S. M. Chung, *Current Appl. Phy.*, 2007, **7**, E6-E10.
- 49 T. Kawai, M. Takemoto, S. Fujibayashi, M. Neo, H. Akiyama, S. Yamaguchi, D. K. Pattanayak, T. Matsushita, T. Nakamura and T. Kokubo, *J. Mater. Sci.: Mater. Med.*, 2012, **23**, 2981-2992.
- 50 Z. Wang, Y. Sun, D. Wang, H. Liu and R. I. Boughton, *Int. J.Nanomedicine*, 2013, **8**, 2903-2916.

### Figure captions

**Fig. 1** Schematic representation of various chemical and thermal treatments.

**Fig. 2** SEM images of Ti metal treated with  $\text{H}_2\text{O}_2$  and subsequently in  $\text{AgNO}_3$  solution of different concentrations.

**Fig. 3** (a) Amount of silver present on the surface as measured by EDX and (b) total amount of silver incorporated into the Ti metal treated with  $\text{H}_2\text{O}_2$  and  $\text{AgNO}_3$  solution of different concentrations as measured by AAS.

**Fig. 4** TEM images and their corresponding SAED pattern of Ti metal treated with  $\text{H}_2\text{O}_2$  and subsequently in  $\text{AgNO}_3$  solution of different concentrations as indicated and subjected to heat treatment.

**Fig. 5** XPS survey spectrum of Ti metal treated with  $\text{H}_2\text{O}_2$  and subsequently in  $\text{AgNO}_3$  solution (0.05 mM) and heat treated at  $600^\circ\text{C}$ . The XPS spectrum for Ag is shown in inset.

**Fig. 6** Raman spectra of Ti metal treated with  $\text{H}_2\text{O}_2$  and subsequently in  $\text{AgNO}_3$  solution of different concentrations.

**Fig. 7** (a) Raman spectra and (b) XRD patterns of Ti metal treated with  $\text{H}_2\text{O}_2$  and subsequently in  $\text{AgNO}_3$  solution of different concentrations and subjected to heat treatment.

**Fig. 8** Silver release study from Ti metal treated with  $\text{H}_2\text{O}_2$  and subsequently in  $\text{AgNO}_3$  solution of concentration as indicated before and after heat treatment in SBF.

**Fig. 9** Antibacterial study of Ti metal treated with  $\text{H}_2\text{O}_2$  and subsequently in  $\text{AgNO}_3$  solution of different concentrations by disk diffusion method (a) before and (b) after heat treatment and (c) direct physical contact method for same set of samples after heat treatment.

**Fig. 10** Mechanism of antibacterial activity of silver from Ti-HP-Ag surface.

**Fig. 11** (a) Cell viability study in MG 63 osteosarcoma cell lines for Ti-HP-Ag surface by MTT assay and (b) a typical cell adhesion study in MG 63 cell lines on Ti-HP-1Ag-H600 surface as observed by SEM.

**Fig. 12** SEM images of Ti metal treated with  $\text{H}_2\text{O}_2$  and subsequently in  $\text{AgNO}_3$  solution of different concentrations subjected to heat treatment and soaked in SBF for 1 and 7 days. Spherical particles deposited on the surface indicate the apatite.

**Fig. 13** XRD results of Ti metal treated with  $\text{H}_2\text{O}_2$  and subsequently in  $\text{AgNO}_3$  solution of different concentrations and heat treatment and soaked in SBF for 7 days.

### Table Captions

**Table. 1** Notations of various chemical treatments.

**Table. 2** The survival number of *Staphylococcus aureus* cells for Ti metal treated with  $\text{H}_2\text{O}_2$  and  $\text{AgNO}_3$  solution of different concentrations and subjected to heat treatment and its bacterial killing efficiency.

**Table 1.**

<b>Chemical treatments</b>	<b>Notations</b>
Untreated Ti metal (as-polished)	Ti
Ti metal treated with 27 % H <sub>2</sub> O <sub>2</sub> solutions, 70°C, 3h	Ti-HP
Ti metal treated with 27 % H <sub>2</sub> O <sub>2</sub> solution 70°C, 3h and 0.05-100 mM AgNO <sub>3</sub> solution, 40°C, 3h	Ti-HP-0.05-100Ag
Ti metal treated with 27 % H <sub>2</sub> O <sub>2</sub> solution 70°C, 3h and 0.05-100 mM AgNO <sub>3</sub> solution, 40°C, 3h and heat treatment 600°C, 1 h	Ti-HP-0.05-100Ag-H600

Table 2.

Sample	CFU/ml	Killing efficiency (%)
Control	$3 \times 10^5$	0
Ti-HP-0.05Ag-H600	$0.318 \times 10^5$	89.4
Ti-HP-1Ag-H600	$0.008 \times 10^5$	99.7
Ti-HP-10Ag-H600	$0.017 \times 10^5$	99.61
Ti-HP-100Ag-H600	$0.008 \times 10^5$	99.7

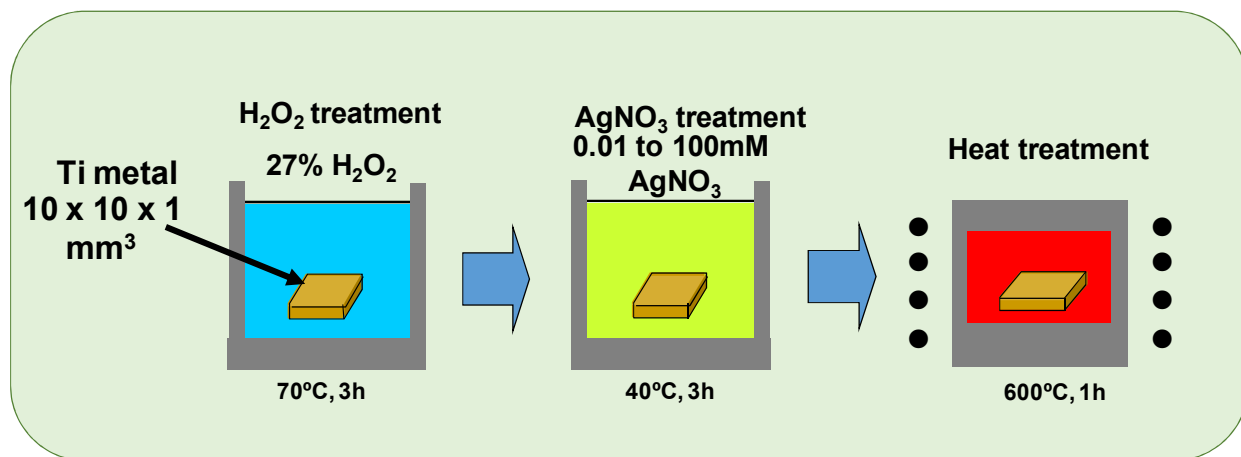


Fig. 1

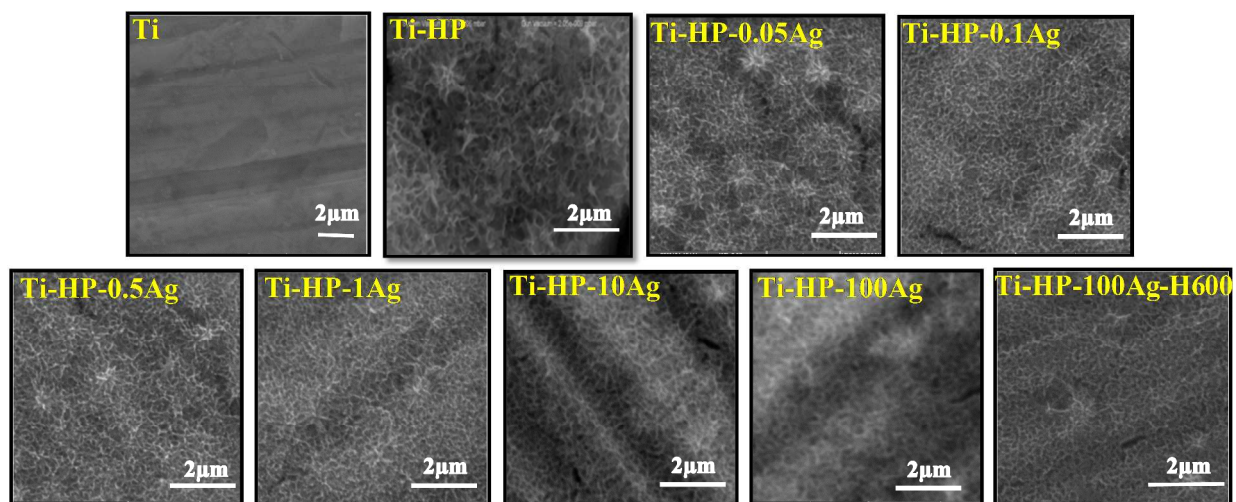


Fig. 2



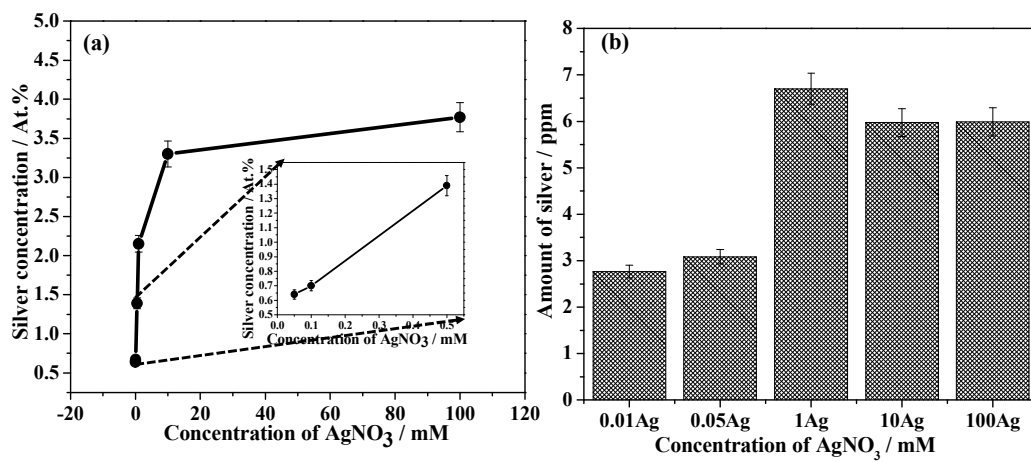


Fig. 3

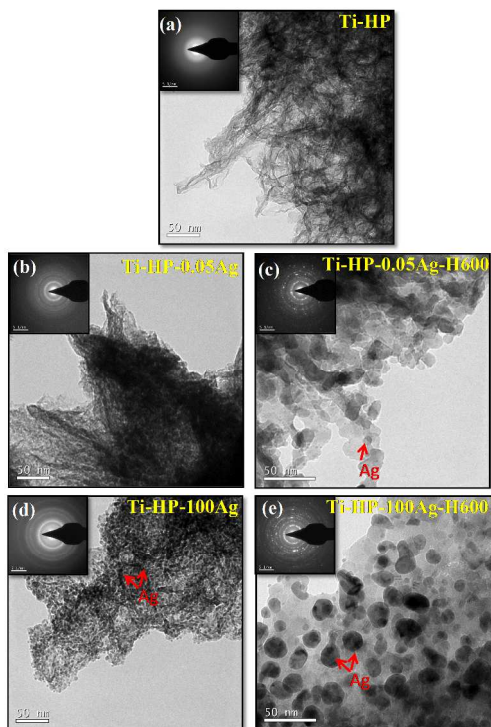


Fig. 4

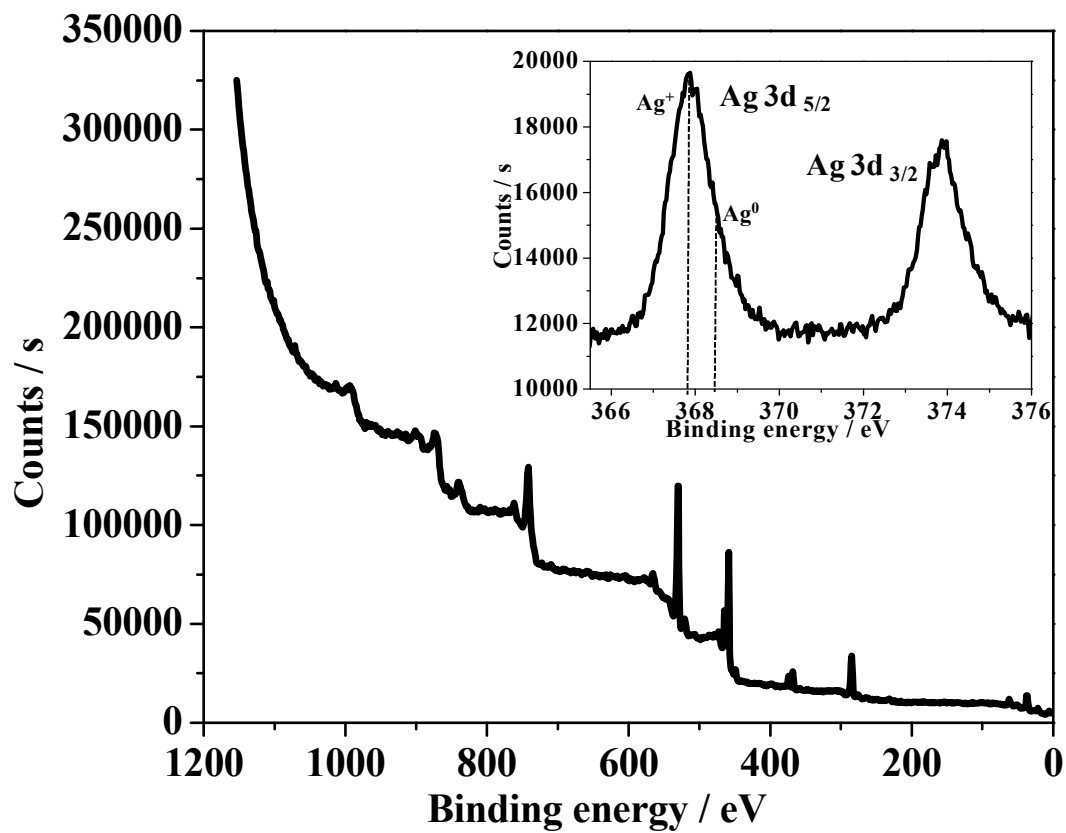


Fig.5

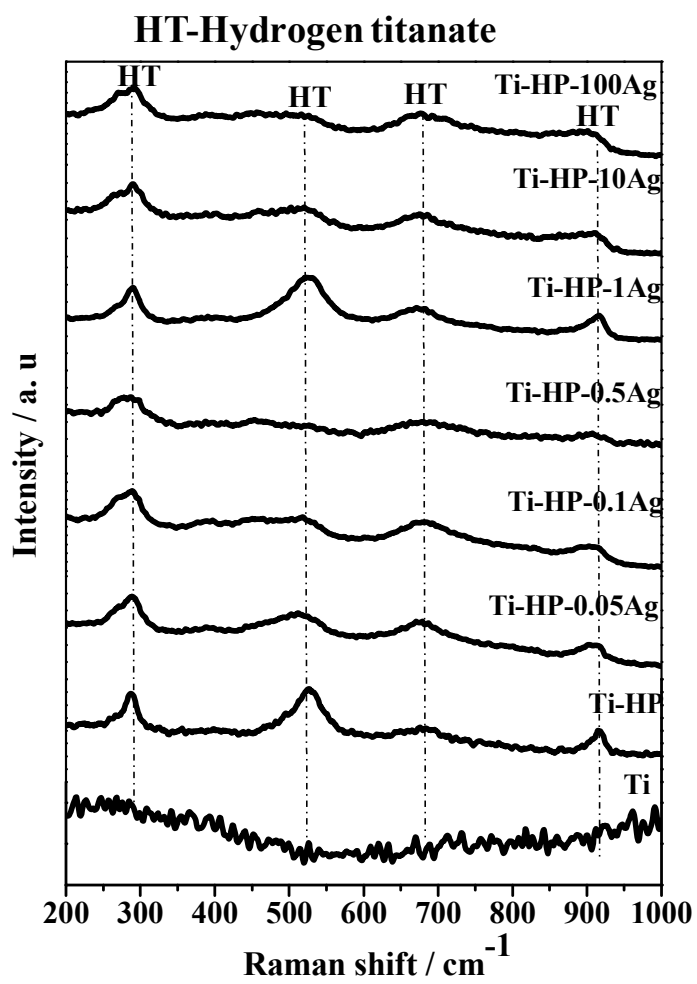


Fig. 6

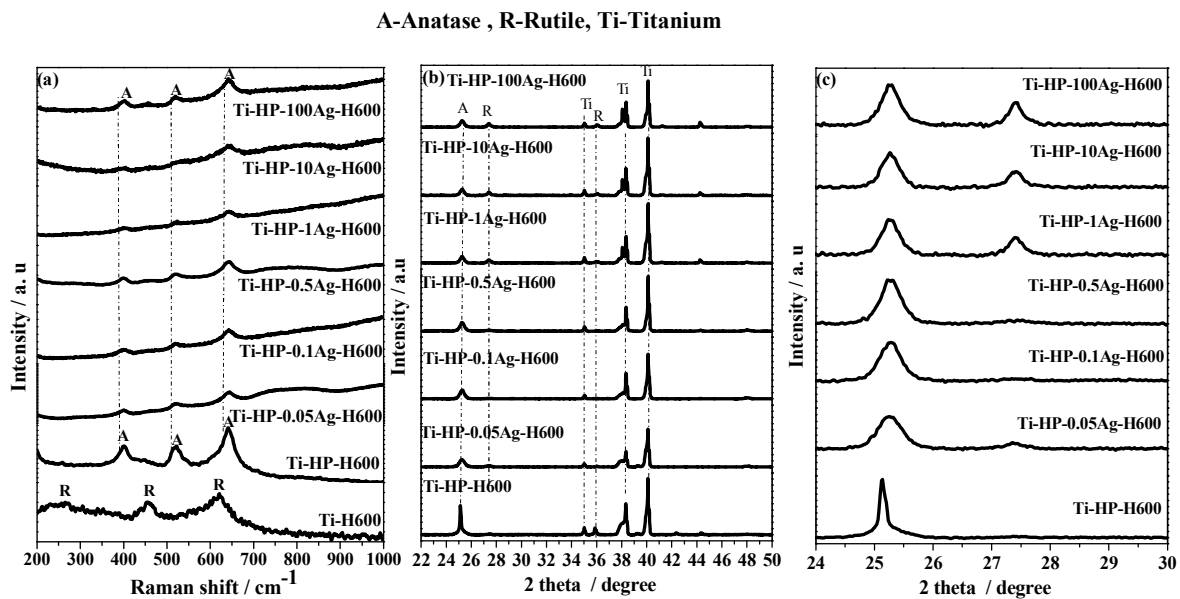


Fig. 7

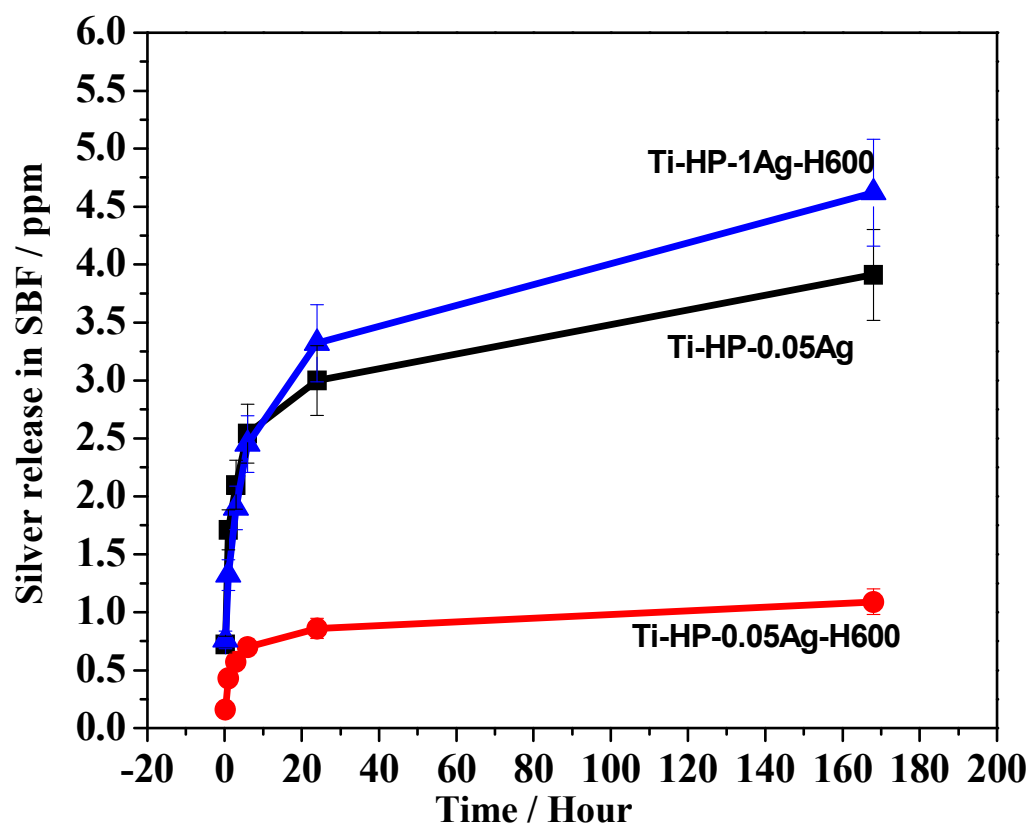


Fig. 8

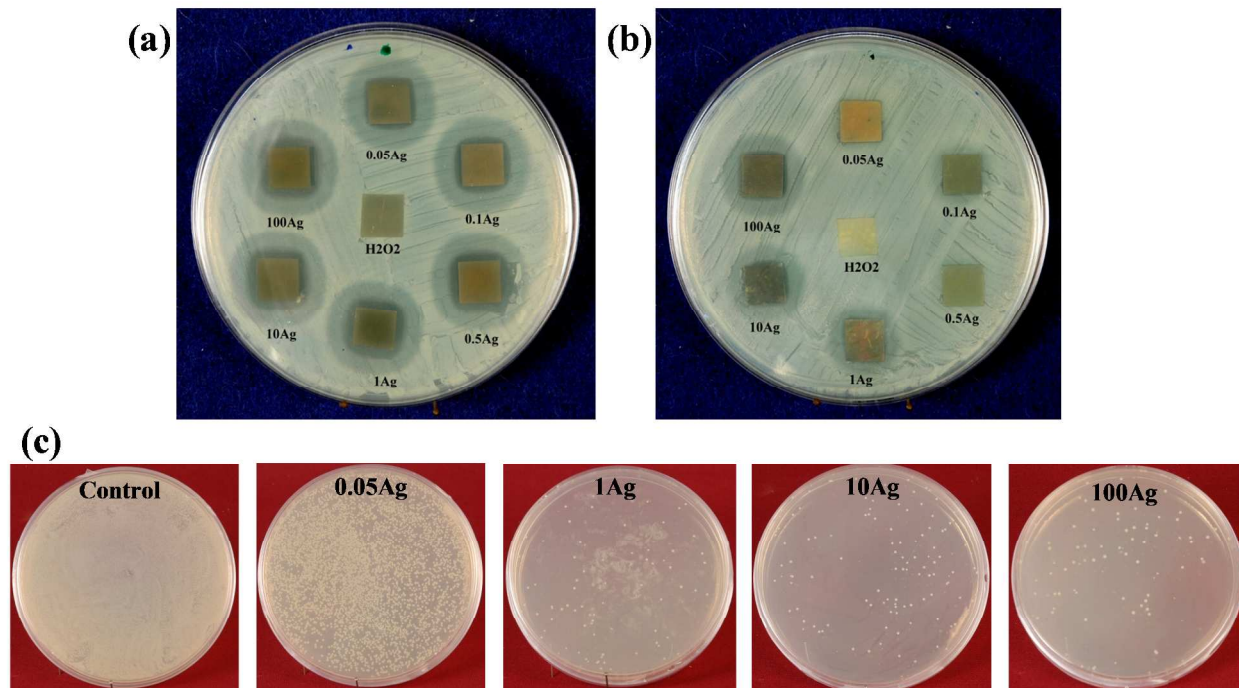


Fig. 9

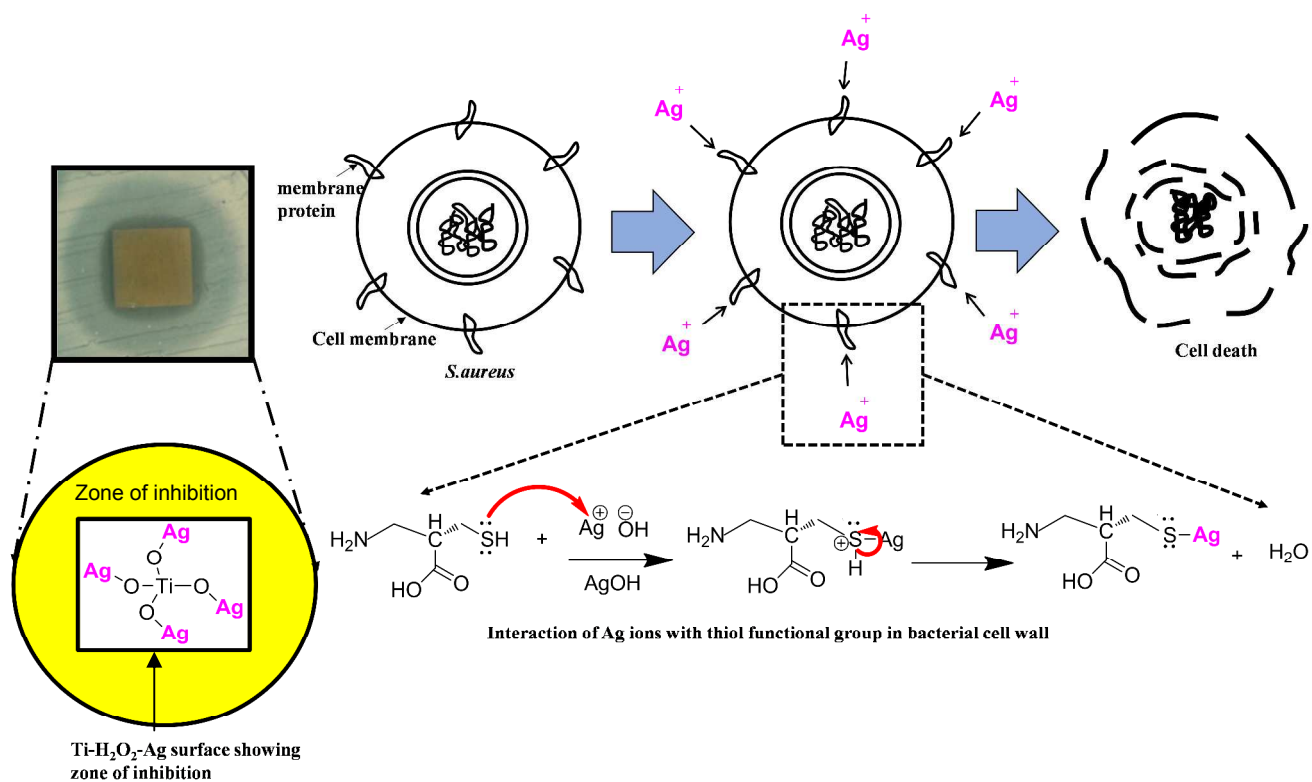


Fig. 10



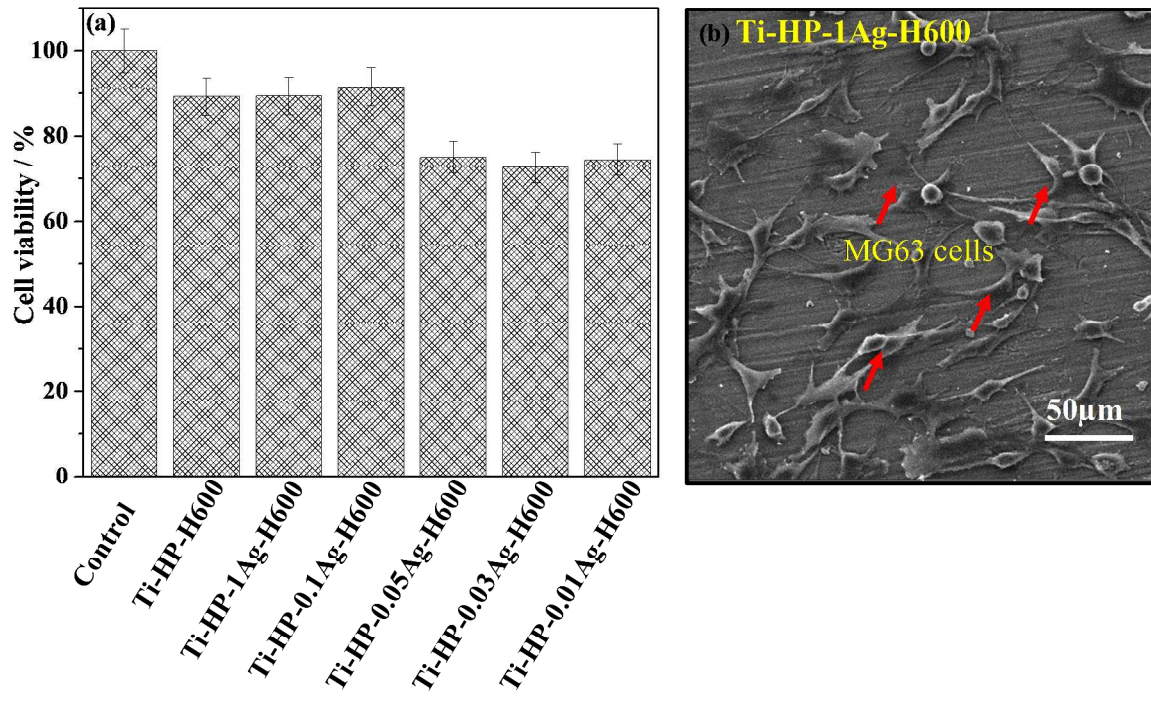


Fig. 11

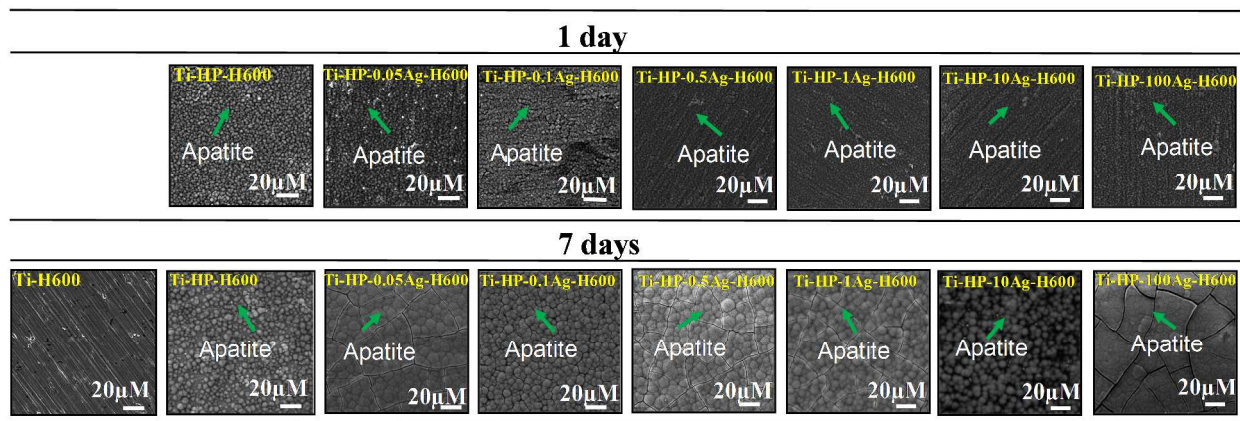


Fig. 12

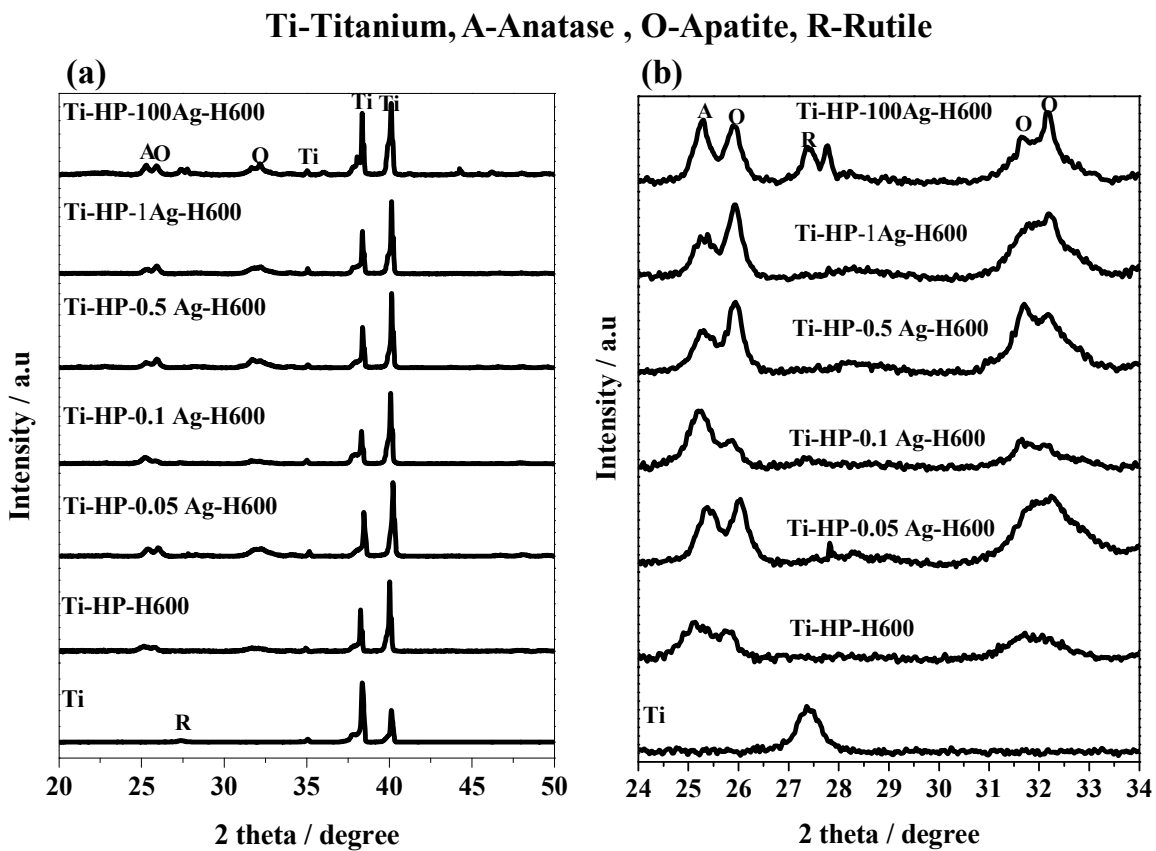


Fig. 13